Online Junction Temperature Extraction of SiC Power MOSFETs With Temperature Sensitive Optic Parameter (TSOP) Approach

Chengmin Li, *Student Member, IEEE*, Haoze Luo, *Member, IEEE*, Chushan Li, *Member, IEEE*, Wuhua Li, *Member, IEEE*, Huan Yang, *Member, IEEE*, and Xiangning He, *Fellow, IEEE*

***Abstract*—Accurate information of the junction temperature of SiC power MOSFETs ensures safe operation and helps reliability assessment of the devices. In this paper, an online junction temperature extraction method is proposed based on the electroluminescence phenomenon of the body diode of SiC power MOSFETs. It is found that during the forward conduction interval of the body diode, visible blue light is emitted around the chip, which ascribes to the radiative recombination in the low doped region of SiC MOSFETs. Experimental results suggest the light intensity changes linearly with the variation of the temperature and behaves as a temperature sensitive optic parameter (TSOP). Further, an electro-thermal-optic model is proposed to reveal the relationship between the electroluminescence intensity, forward current, and junction temperature. Based on the TSOP, an online junction temperature extraction method is proposed for SiC MOSFETs and verified in an SiC MOSFET based inverter. Compared with state-of-the-art methods, the proposed junction temperature measurement method is contactless and immune from the aging of the package.**

***Index Terms*—Body diode of SiC MOSFETs, electroluminescence, junction temperature extraction, thermal management.**

I. Introduction

SIC power MOSFETs are emerging next generation devices for the high switching frequency, high voltage, and high temperature converters. As the successful commercialization of the wide band gap devices, the SiC power MOSFETs based applications are growing gradually. To date, although SiC devices are meant to operate in high temperature, their maximum junction temperature is limited by the package and relatively small die

Manuscript received October 7, 2018; accepted December 24, 2018. Date of publication January 10, 2019; date of current version June 28, 2019. This work was supported in part by the National Key Research and Development Program of China under Grant 2017YFE0112400, in part by the National Nature Science Foundations of China under Grants 51677166 and 51877192, and in part by the Zhejiang Provincial Natural Science Foundation under Grant LR16E070001. Recommended for publication by Associate Editor M. Nawaz. *(Corresponding author: Wuhua Li.)*

C. Li, H. Luo, W. Li, H. Yang, and X. He are with the College of Electrical Engineering, Zhejiang University, Hangzhou 310027, China (e-mail:

-

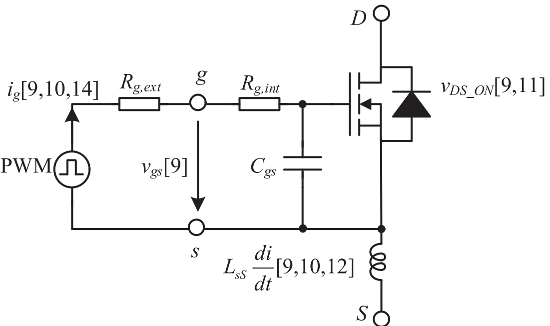

Fig. 1. TSEPs of SiC power MOSFETs.

These parameters have been proved to estimate the junction temperature successfully.

However, from application perspective, there are two main challenges in junction temperature sensing with TSEPs. On one hand, the temperature estimation and the ongoing aging of the package are deeply coupled and difficult to be separated [15]. On the other hand, the electrical signals may be disturbed by the high EMI environments, especially for those measurements with the physical contacts [11]. This is the case especially for SiC power MOSFETs with fast switching speed. High *dv/dt* and *di/dt* introduces high noise to the sampling circuit. The fast switching speed also add more difficulty in designing the sampling unit for some TSEPs, for example, the gate driver current [16] and the drive threshold voltage V_{th} measurement method [11]. To overcome these limits, it is of great significance to search new indicators of the junction temperature of the devices.

Generally, the SiC crystal has the electroluminescence feature and is adopted to fabricate light emitting diode (LED) in history [17]. However, the incidental light emitting phenomenon in the body diode of SiC power MOSFETs has not drawn any attention yet. In the latest generation of the SiC MOSFET, the body diode is suggested to conduct the load current during the dead-time instead of the SBDs [18]–[21]. During forward conduction of the body diode, it is found that a blue light is generated from the SiC chip. This phenomenon has been briefly reported in [22] and is utilized in current sensing. In this paper, the electroluminescence of the commercialized SiC MOSFETs is investigated and characterized in detail. From the point view of reliability, it is found out that the luminescence intensity is a thermal sensitive optic parameter (TSOP). A light detection circuit using the widely adopted photodiode is designed to transfer the generated light into the electrical signals. And then this method is adopted in a real converter that the body diode is only conducted during the dead time. The analytical model is proposed considering the PWM switching. Based on the proposed model, junction temperature can thus be estimated online.

This paper is organized as follows, in Section II, the mechanism of the electroluminescence is analyzed to give a basic understanding. In Section III, the temperature dependence of the luminescence is investigated and TSOP method is proposed. In Section IV, the electroluminescence in a PWM inverter is analyzed and modeled. In Section V, the TSOP based junction temperature extraction method is verified in an experimental platform. Finally, the conclusions of the TSOP method are provided in Section VI.

II. Mechanism of Electroluminescence Phenomenon of SiC MOSFET Body Diode

Electroluminescence phenomenon refers to the photo emission from a solid-state material caused by an electrical power source excitation [17]. The visible light emission from the SiC material has been reported more than 100 years ago. The first light emission diode (LED) made from SiC has been introduced based on this phenomenon. But it is soon eliminated due to the low light generation efficiency. In this section, the electroluminescence of the body diode of the SiC power MOSFETs is observed and characterized.

SiC power MOSFETs have an intrinsic *p-i-n* body diode operate in the bipolar conduction mode. Fig. 2(a) demonstrates an example of the conduction of the body diode in a half bridge configuration, when the lower MOSFET turns OFF, the body diode of the upper switch will turn ON to freewheel the load current. During the forward conduction of the body diode, the electros and holes are injected into the low doped region of the SiC MOSFET, as depicted in Fig. 2(b). Fig. 2(c) demonstrates the excess carrier distribution in the low doped region [23]. In the equilibrium state, the injection and recombination of the excess carriers are balanced. In the recombination process, the extra energy may be released in the form of a photon [23].

There are three kinds of recombination in the low doped region of the SiC MOSFET chip, as depicted in Fig. 3. The direct band to band recombination occurs when the free electros drop to the valence band directly. The defect assisted recombination refers to the recombination through the energy level in the forbidden band. The auger recombination refers to the free electros falls into the valence band, but the extra energy is transferred to another free carrier. In the SiC *p-i-n* diode, the dominant recombination in the normal operation is the defect energy level states assisted recombination [24].

The radiative recombination, within which the recombination is accompanied by a photon emission, is possible to occur in the band to band recombination and deep-level states assisted recombination [17]. Since the extra energy in the recombination process is released by a photon, the relationship between the peak wavelength λ of the light and energy E is [25]

$$\lambda = \frac{1240}{E}\mathrm{nm}. \quad (1)$$

The energy of the photon emitted from the direct band to band recombination satisfies

$$E = E_g \quad (2)$$

where E_g is the energy bandgap of the 4H-SiC. The bandgap of 4H-SiC is 3.26 eV at 300 K, from (1), the peak wavelength of the released light is 380 nm, which is near the wavelength range of blue light.

Another radiative recombination mechanism is through the deep level states in the forbidden band. There exist many deep level states in the forbidden band of the SiC materials. Some of these deep level states are electrically activated and act as

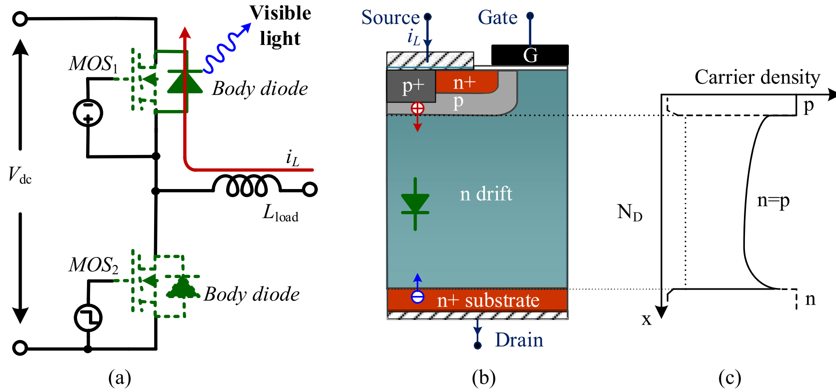

Fig. 2. Bipolar conduction in bode diode of SiC power MOSFET. (a) Current commutation of half bridge leg. (b) Structure of SiC MOSFETs. (c) Excess carrier distribution in the body diode.

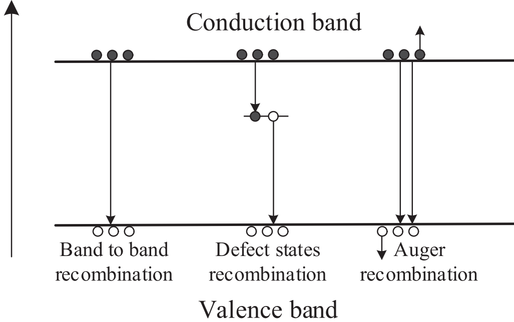

Fig. 3. Recombination in low doped region of SiC power MOSFET.

TABLE I
ELECTROLUMINESCENCE PHENOMENON IN SiC MOSFETs

Device	Decapsulated SiC MOSFETs	Luminescence of body diode at 15A
Rohm 1200V/72A SCT3030KL		
CREE 1200V/90A C2M0025120D		

radiative recombination centers [24], [26]. In the recombination, the energy of the generated photon is smaller than the bandgap. As a result, the released peak wavelength is larger than 380 nm.

To further understand the origin of the light emission, the spectrum of the generated light is measured. Since the chip of the commercial SiC MOSFETs is packaged and cannot be observed directly, to measure the status of the chip directly, two TO247 MOSFETs from two suppliers are decapsulated, as listed in Table I. When the body diode is forward conducted, an obvious blue light is generated around the SiC MOSFET chip.

To measure the spectrum of the emission light, an experimental platform is designed, as shown in Fig. 4. The body diode of

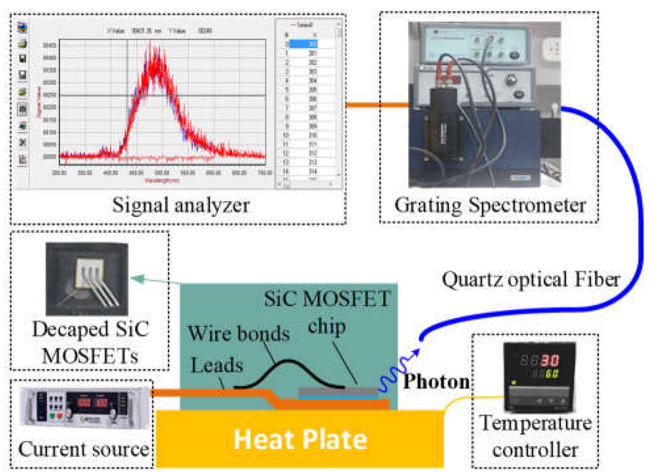

Fig. 4. Experimental platform setup for spectrum measurement.

the SiC power MOSFET is conducted by a controllable current source. The generated light is exported to an optic grating spectrometer by a quartz optic fiber placed aside the SiC MOSFET chip. Since the body diode has relatively large power loss during continues conduction [27], the self-heating of the devices needs to be considered. To decouple the influence of forward current and the junction temperature on the light intensity, a heating plate is placed under the SiC MOSFET to compensate the junction temperature difference at different forward current conditions.

Fig. 5 plots the unified light spectrum of the two MOSFETs from different vendors at 100 °C. In 300–700 nm spectrum range there are only two main peak wavelengths, accordingly 383 nm, 485 nm. Interestingly, through the two MOSFETs fabricated by different vendors, the peak wavelength is the same, which indicates the same light generation mechanism. Calculating the recombination energy level using (1), the corresponding radiative recombination energy level is 3.23 eV and 2.56 eV. The 3.23 eV photon equals to the energy bandgap of the 4H-SiC, thus is caused by the direct band to band recombination. The 2.56 eV photon is 0.68 eV below the bandgap and released by the deep energy level assisted recombination.

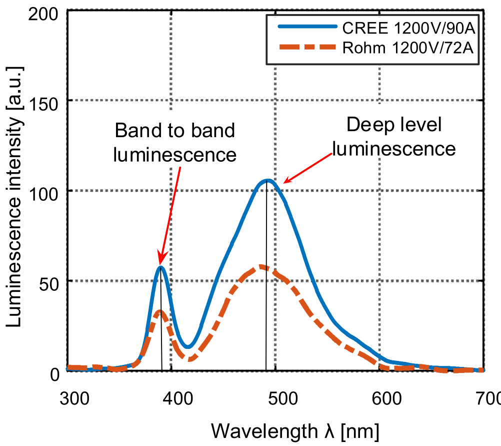

Fig. 5. Spectrum of generated light at 15 A/100 °C.

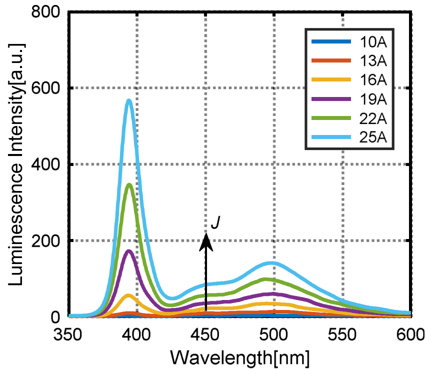

Fig. 6. Luminescence intensity under different forward currents at 120 °C.

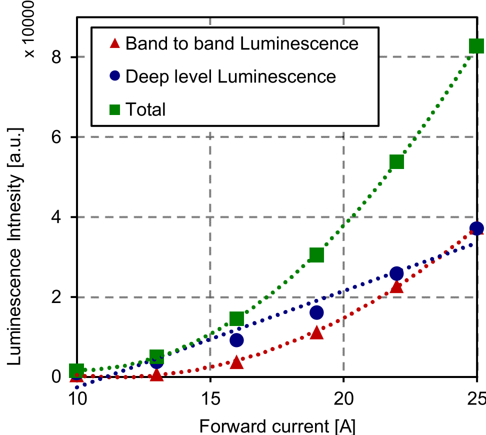

Fig. 7. Forward current dependence of light intensity.

Furthermore, it is found that the energy level of defect $Z_{1/2}$ in 4H-SiC, located at the conduction band below 0.63-0.68 eV [26] matches very well from the measured 2.56 eV photon. Therefore, the measured waveform is most likely from the radiative recombination in the $Z_{1/2}$ deep level states. The defect $Z_{1/2}$ in 4H-SiC is a common intrinsic type of defect, which means it is stable and can be found in all the SiC power MOSFETs [28].

Based on the aforementioned analysis, for devices from different manufactures, the light generation mechanism is the same. Thus, this stable electroluminescence phenomenon is very suitable to be used as an indicator reflecting the operation status of the SiC MOSFET chip.

III. Junction Temperature Dependence of Luminescence Intensity

According to the previous analysis, the radiative recombination in the body diode of the SiC power MOSFET composes of the direct band to band recombination and indirect deep level states participated recombination. For the light wavelength center at 383 nm, the direct band to band recombination rate R_{direct} has the form [29]

$$R_{\text{direct}} = Bn^2 \tag{3}$$

where B is the direct recombination probability, n is the excess carrier concentration in the low doped region of SiC MOSFETs. For the light wavelength center at 485 nm, the indirect recombination rate R_{indirect}, has the form [29]

$$R_{\text{indirect}} = An \tag{4}$$

where A is the indirect recombination probability. Under the high-level injection condition at a given temperature, the excess carrier density n is proportional to the forward current i [23]

$$n \propto i\tau_{\text{HL}} \tag{5}$$

where τ_{HL} is the excess carrier life time. The total light intensity I_{EL} is proportional to the band to band radiative recombination rate and the deep level radiative recombination rate [30], yields

$$I_{\text{EL}} \propto I_{\text{indirect}} + I_{\text{direct}} = An + Bn^2. \tag{6}$$

Therefore, the relationship between the light intensity and the forward current i can be represented as

$$I_{\text{EL}} = ai + bi^2 \tag{7}$$

where a, b are coefficients influenced by junction temperature. To verify (7), a series of light spectrum is measured form 10 A to 25 A with the CREE SiC power MOSFET at a given temperature. When the forward current is 25 A, the total power loss of the studied SiC power MOSFET is around 65 W. In this condition, the junction temperature due to self-heating is 120 °C. Thus, the measurement is conducted under 120 °C conditions.

The measured spectrum of luminescence is demonstrated in Fig. 6. As the forward current increases, the luminescence intensity increases. Meanwhile, the increasing speed of band to band luminescence is faster than the deep level luminescence. Fig. 7 gives the statistic light intensity for different kinds of the luminescence. The measured data suggests the band to band light intensity increases quadratically with the forward current. And the deep level light intensity increases linearly with the forward current. The growing trend matches well with the theoretical analysis in (7). Besides, the similar measured curve of the current dependence of the total luminescence is also reported in [22].

Aforementioned analysis assumes that the junction temperature remains constant under different forward currents. Whereas the light intensity changes with the junction temperature in

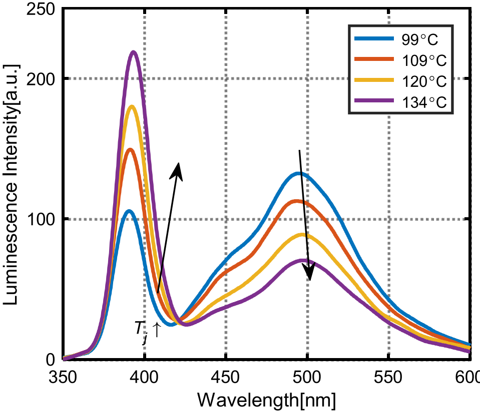

Fig. 8. Luminescence intensity under different temperatures at 20 A.

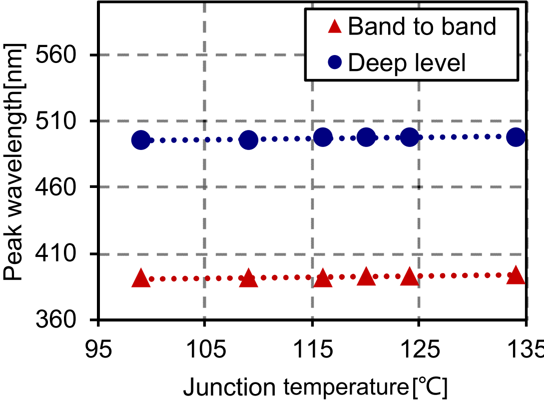

Fig. 9. Temperature dependence of peak wavelength.

reality and the temperature should be considered. In Fig. 8, a series of light spectrum is measured at the forward current 20 A in the CREE SiC power MOSFET. Apparently, the band to band luminescence increases with the increasing junction temperature, whereas the deep level luminescence decreases with the increasing junction temperature. There are many influential factors contributes to the temperature dependence of the luminescence intensity. In summary, the light emission efficiency changes with the temperature due to the following reasons:

1) As the temperature increases, the energy bandgap of the semiconductors decreases, for 4H-SiC material, the energy bandgap satisfies [31]

$$E_g = 3.263 - 3.3 \times 10^{-4} (T - 300K) \tag{8}$$

where T is the temperature. Since the energy bandgap decreases with the temperature increase, the peak wavelength increases slightly as the junction temperature increases, as measured in Fig. 9.

2) The excess carrier lifetime increases with the junction temperature [32]. In SiC materials, the carrier lifetime is

$$\tau_{\mathrm{HL}} = \tau_0 \left(\frac{T}{300K}\right)^{1.72}. \tag{9}$$

When the junction temperature increases, the carrier lifetime increases, as shown in (5), the radiative recombination rate will change accordingly. As a result, the luminescence intensity is affected.

3) The recombination probability also changes with the junction temperature. The band to band recombination probability increase with the junction temperature, and the deep level recombination probability decreases with junction temperature [29].

4) Partial generated photon will be absorbed again and the amount increase with the junction temperature [17].

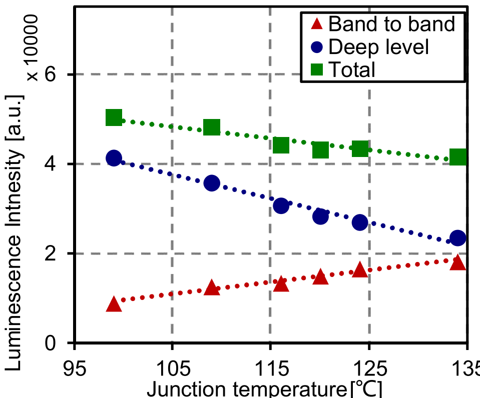

Fig. 10. Temperature dependence of luminescence intensity at 20 A with CREE SiC power MOSFET.

Due to above reasons, the analytical expression of the temperature dependence of the light intensity is complex. Whereas near the operating temperature of the SiC power MOSFETs, the light intensity is enough to be described by a linear phenomenological equation [17]. Fig. 10 demonstrates the temperature dependence of the light intensity at 20 A with the CREE SiC power MOSFET. In the measured data, it is verified that both the band to band luminescence and deep level luminescence changes linearly with the junction temperature. The calculated linear correlation coefficient is larger than 0.98, which demonstrates a highly linear dependence between the junction temperature and the light intensity.

Since the band to band luminescence and deep level luminescence demonstrate different temperature dependent coefficients, the total light intensity is

$$I_{\mathrm{EL}} = I_{\mathrm{indirect}} [1 + k_1 \Delta T] + I_{\mathrm{direct}} [1 + k_2 \Delta T] \tag{10}$$

where I_{direct} and I_{indirect} are the light intensity of the band to band luminescence and the deep level luminescence at a given temperature, k_1 and k_2 are constant coefficients, and ΔT is the junction temperature variation. Based on the previous analysis, at a given junction temperature, the light intensity is only related to the forward current, combing (7) and (10), the total light intensity is

$$I_{\mathrm{EL}} = a_0 i [1 + k_1 \Delta T] + b_0 i^2 [1 + k_2 \Delta T]. \tag{11}$$

This electro-thermal-optic equation links the junction temperature, the forward current and output light intensity. The light intensity demonstrates a good linearity with the junction temperature. Thus, the light intensity serves as a temperature sensitive

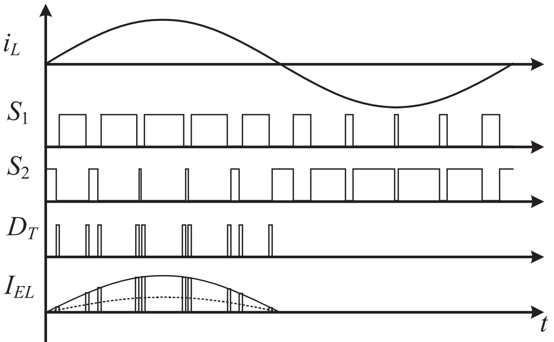

Fig. 11. Waveforms of electroluminescence in a SiC inverter.

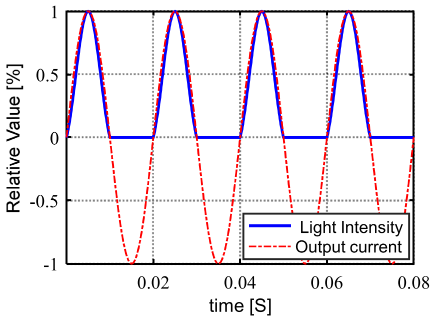

Fig. 12. An example of light intensity in a PWM converter.

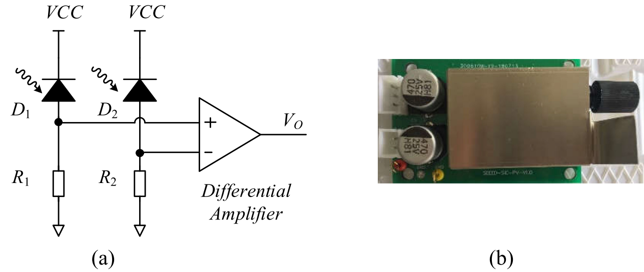

Fig. 13. Schematic (a) and prototype (b) of the photosensitive circuit.

optic parameter (TSOP) that reflect the junction temperature of the SiC chips.

IV. Electroluminescence Analysis in PWM Converters

Previous analysis is based on the continue forward current conduction in the body diode, however, in most applications, the body diode is only conducted during the dead-time interval. Under this condition, the luminescence phenomenon is also existed in the SiC MOSFET based inverter. This section will give a detail discussion taking a half bridge leg as an example. In the SiC converters, the synchronous rectification of the SiC MOSFET is suggested to replace the conduction of the body diode to reduce the ON-State loss. As a result, the body diode is only conducted in the dead time period, as depicted in Fig. 2(a). Fig. 11 depicts the modulation scheme of a two level SiC MOSFET inverter.

To SiC MOSFET inverter, the ripple current of the inductor is relatively small. Ignoring the ripple current of the inductor, the load current is

$$i_L = I_L \sin(\omega t) \tag{12}$$

where I_L is the magnitude of the load current, ω is the fundamental angular frequency. In the voltage source PWM inverter, a small piece of time is inserted between the turn ON and OFF of the devices to ensure the reliable current commutation between the upper and lower switch. If the load current is positive, when the lower switch is turned ON/OFF, the body diode of the upper switch will be conducted until the deadtime ends, as demonstrated in Fig. 11. Two pieces of pulse current flow through body diode in a switching period in this case. As a result, the emitted light is composed of a series of the optic pulses. If the load current is negative, the body diode will not be conducted.

To simplify the analysis, the turn ON and turn OFF transition of the body diode is ignored due to the fast switching time. During the dead time, the current of the body diode equals the load current. Thus, the average light intensity in a switching period can be calculated by

$$i_{\mathrm{EL}} = \frac{2}{T_S} \int_t^{t+T_D} \left(a_0 i_L(\tau)(1 + k_1 \Delta T) + b_0 i_L^2(\tau)(1 + k_2 \Delta T)\right) d\tau \tag{13}$$

where T_D is the deadtime, T_S is the switching period. Since the deadtime is relatively small compared with the fundamental frequency, the load current can be approximated constantly during the deadtime, yields

$$i_{\mathrm{EL}} = d_{\mathrm{DT}} \left(a_0 i_L (1 + k_1 \Delta T) + b_0 i_L^2 (1 + k_2 \Delta T)\right) \tag{14}$$

where the deadtime duty cycle d_{DT} is

$$d_{\mathrm{DT}} = \frac{2T_D}{T_S}. \tag{15}$$

Fig. 12 gives an example of the ideal light intensity and the forward current of a SiC MOSFET body diode at a constant junction temperature condition. For a given PWM converter, the deadtime is constant during normal operation, the load current is sampled by a current sensor. Adopting (14), the junction temperature can be calculated instantaneously.

V. Experimental Verification

To estimate the junction temperature of the SiC power MOSFETs based on TSOP, the generated light should be detected first of all. Fortunately, photosensitive devices have been widely adopted in industry. In this section, a photosensitive circuit is designed and verifies in reality. Then the TSOP estimation method is verified in a 5 kVA SiC inverter.

A. Photo Sensitive Circuit Design

The photodiode SFH250 V [33] is adopted to detect the light form the SiC power MOSFET. When applied by a reverse voltage, the current of the photodiode is proportional to the input luminous flux. The detection circuit is demonstrated in Fig. 13(a). To eliminate the stray light from the environment, two photodiodes

TABLE II
SPECIFICATIONS OF SiC INVERTER

Specifications	Value
Input voltage V_{in}	400V
Output Voltage V_o	220VAC
Switching frequency f_s	50kHz
Load inductance	0.8mH
Deadtime	300ns

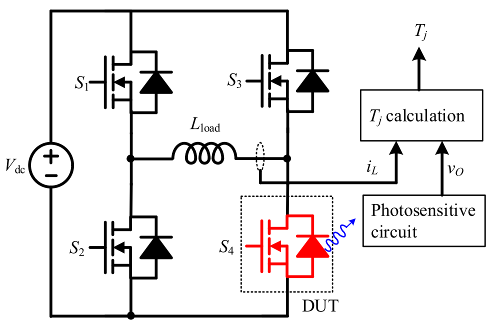

Fig. 14. Block diagram of junction temperature extraction setup.

with the differential amplifier is adopted. D_1 measures the light generated by SiC power MOSFET and the auxiliary diode D_2 measures the environment light near the SiC chip. The output voltage v_o of the sampling circuit is proportional to the input light intensity, that is

$$v_O = k i_{\mathrm{EL}} \tag{16}$$

where i_{EL} is the light intensity, k is the proportional coefficient. A quartz optic fiber is placed besides the SiC chip to export the generated light to the sense circuit. To avoid the disturbance from the ambient, a metal shield is added to the sampling circuit, as demonstrated in Fig. 13(b).

B. Experimental Platform Setup

A full bridge SiC inverter based on CREE 1200 V/90 A SiC power MOSFETs is built to verify the proposed junction temperature estimation method. The key parameters of the SiC inverter are listed in Table II. The switching frequency is 50 kHz and the load inductor is 0.8 mH. Fig. 14 demonstrates the diagram of the experimental setup. To measure the generated light in the package, the lower switch S_4 is decapsulated and acts as the device under test (DUT).

Fig. 15 demonstrates the experimental platform setup. The dc power supply offers a constant voltage or current to the converter. The fiber optic temperature thermometer OTG-F from Opsens Solutions [34], which has ± 0.8 °C resolution and 5 ms response speed, is adopted as the accurate measurement reference of the temperature. Since the light flux exported to the photodiode is affected by the position of the optic fiber, a 3-axis precision displacement platform is adopted to stabilize the optic fiber. Fig. 16 demonstrates the light generation phenomenon when the output current equals 25 A during normal switching of the devices. Compared with the light generation in Table II, this emission light is generated in the switching operation of the devices when the body diode is only conducted during the deadtime interval.

C. Test in the Continuous Forward Current Condition

In this section, continuous current is applied to the body diode, then the junction temperature is measured in the thermal steady state. Under different forward currents, the steady state junction temperature is different due to different power loss. By adjusting the cooling fan speed, the output voltage of photodiode sampling circuit is acquired under different junction temperatures at given forward current. The result is demonstrated in Fig. 17. The output voltage decreases linearly with the junction temperature rises.

To realize online junction temperature calculation, the four parameters a_0, b_0, k_1, k_2 need to be obtained first. For a given SiC converter and measurement circuit, these parameters are fixed. Therefore, they can be acquired in a calibrating experiment offline. A series of known junction temperatures, forward currents and output sampling voltage are measured before the normal inverting operation of the converter. According to the electro-thermal-optic model in (11), using linear regression analysis form the measured data, the output voltage is

$$\begin{aligned} v_O = &\, 5.5982 i_L \left(1 - 0.00570 \times \Delta T\right) \\ &+ 0.0178 i_L^2 \left(1 + 0.0155 \times \Delta T\right) \mathrm{mV} \end{aligned} \tag{17}$$

where i_L is the load current, ΔT is the junction temperature variation. The parameters $k_1 = -0.00570$, $k_2 = 0.0155$ indicate the influences of the junction temperature variation on the light generation efficiency of the body diode. In this setup, for band to band luminescence, the light generation efficiency increases 155% when the junction temperature rises 100 °C. And for the deep level luminescence, the light generation efficiency decreases 57% when the junction temperature rises 100 °C. From (17), let $\Delta T = 1.0$ °C, the sensitivity of the junction temperature measurement is

$$\Delta v = \left(-0.0319 i_L + 0.002759 i_L^2\right) \mathrm{mV/^\circ C}. \tag{18}$$

The accuracy of the junction temperature dependent is decided by the forward current and the gain of the measuring circuit. For example, when the forward current equals 30 A, the temperature sensitivity is 1.53 mV/°C.

Further, a step current is added to the body diode, the waveform is demonstrated in Fig. 18. The sensor output voltage responses immediately the current applied, meanwhile the junction temperature rises slowly due to the heat accumulation. Therefore, the output sampling voltage will decrease along with the junction temperature increasing. Using the measured coefficients from (17), the junction temperature is calculated online. The result is demonstrated in Fig. 18. The extracted junction temperature demonstrates a highly coincidence with the measured data from the optic fiber thermometer. The average error is less than ±3 °C.

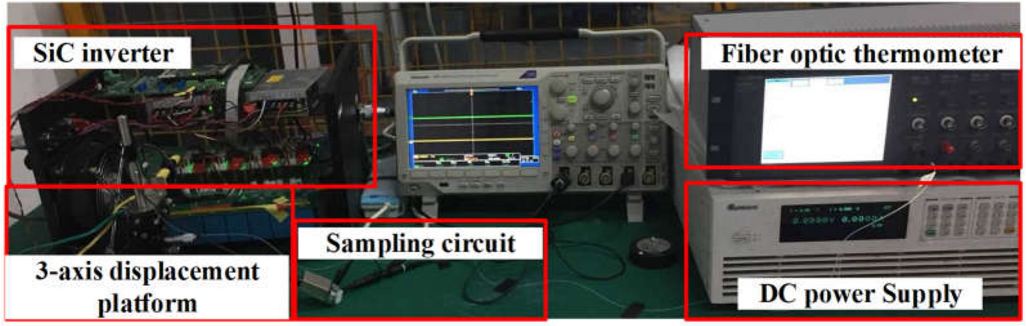

Fig. 15. Appearance of SiC 5 kW inverter platform.

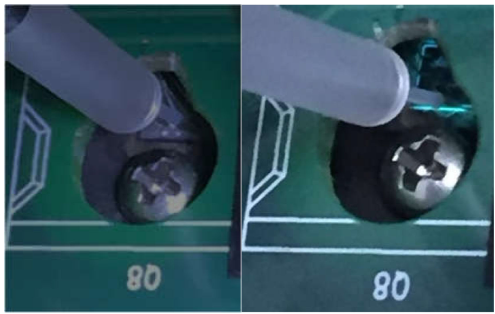

Fig. 16. Demonstration of electroluminescence during switching operation at 25 ARMS.

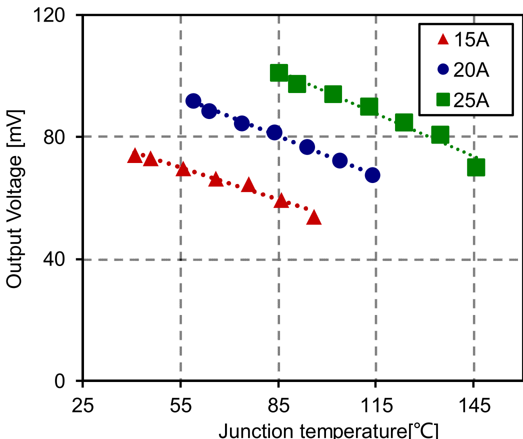

Fig. 17. Junction temperature dependence of sensor output voltage.

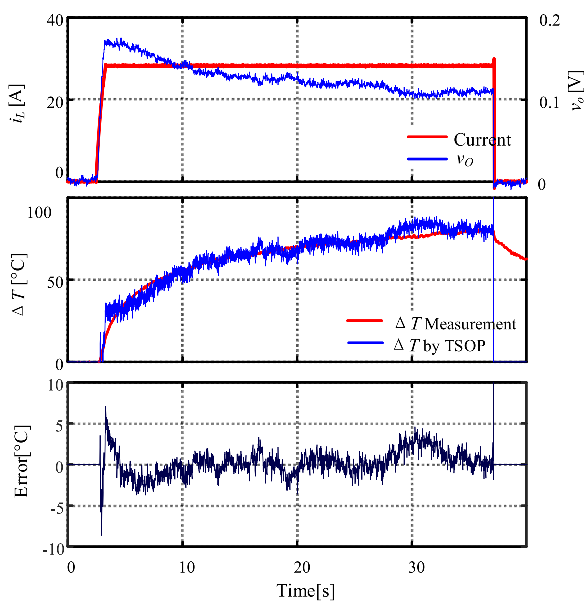

Fig. 18. TSOP method at a current step response.

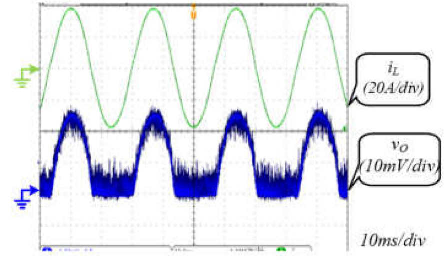

Fig. 19. Waveform of inductor current and sampling circuit output.

D. Online Junction Temperature Measurement in a PWM Inverter

During inverting operation of the SiC converter, the light emission is measured by the sampling circuit in this section. As pictured in Fig. 11, in a fundamental cycle, the body diode of the DUT is only conducted when the load current is larger than zero. Fig. 19 demonstrates the optic sampling output voltage v_o and the load current i_L at 25 A. The output voltage of the photosensitive circuit matches well with the theoretical waveform proposed in Fig. 12.

Using the output voltage and inductor current, the junction temperature can be estimated using (17). Fig. 20 demonstrates the estimated junction temperature with the proposed TSOP. Due to the light is generated in the positive half cycle of the output current, the junction temperature can only be obtained in the positive half cycle. The temperature variation in the negative half cycle cannot be acquired in this setup. The measured junction temperature variation from the fiber optic thermometer is 52 °C. In the positive half cycle of the load current, the error between the TSOP and the measurement from optic fiber thermometer is less than ±5 °C.

The proposed TSOP method demonstrates some good performances such as galvanic isolation and free from the influence of the aging of the package, which are the main challenges in the present online junction temperature extraction methods. The junction temperature estimation unit can be integrated with

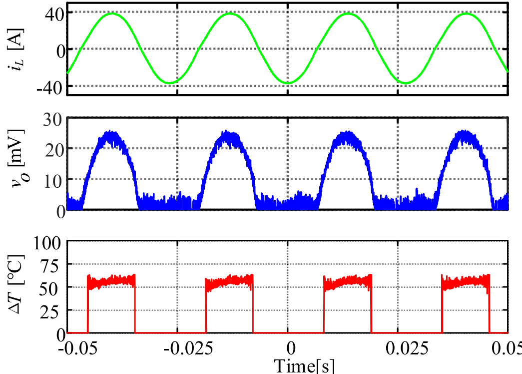

Fig. 20. Estimated junction temperature with proposed DTSOP.

the control unit of the converter. Meanwhile, there exists some drawbacks to overcome, such as the relatively lower sensitivity. The potential improvements including use more sensitive photodiode in the spectrum range of the generated light and select the optimized gain for the amplifier.

VI. Conclusion

The electroluminescence contains information of the inner status of the SiC MOSFETs and can be utilized to develop junction temperature sensing methods. It is existed in all the SiC MOSFETs and has stable characteristics. The luminescence is generated through band to band recombination with 3.23 eV photon emission and deep level recombination with 2.58 eV photon emission. The band to band luminescence increases linearly with the forward current increasing, whereas the deep level luminescence increases quadratically with forward current increasing. Meanwhile, the light intensity demonstrates a good linearity with the junction temperature variation. For the proposed experimental setup, the band to band luminescence increases about 155% with 100 °C temperature increase, the deep level luminescence decreases about 57% with 100 °C temperature increase. Following these discoveries, the TSOP based online junction temperature measurement method is developed and verified in experiments on a 5 kVA SiC inverter. The total error of the TSOP based method during switching operation of the inverter is less than ±5 °C. Moreover, the temperature measurement is contactless and the isolation and electromagnetic interferences are free of concern. To adopt the proposed method, some considerations in package need to be added to the current device package in the future work.

References

[1] K. Sheng, "Maximum junction temperatures of SiC power devices," *IEEE Trans. Electron. Devices*, vol. 56, no. 2, pp. 337–342, Feb. 2009.

[2] B. Hull *et al.*, "Reliability and stability of SiC power MOSFETs and Next-Generation SiC MOSFETs," in *Proc. IEEE Workshop Wide Bandgap Power Devices Appl.*, 2014, pp. 139–142.

[3] U. M. Choi, F. Blaabjerg, and K. B. Lee, "Study and handling methods of power IGBT module failures in power electronic converter systems," *IEEE Trans. Power Electron.*, vol. 30, no. 5, pp. 2517–2533. May 2015.

[4] H. Oh, B. Han, P. McCluskey, C. Han, and B. D. Youn, "Physics-of failure, condition monitoring, and prognostics of insulated gate bipolar transistor modules: A review," *IEEE Trans. Power Electron.*, vol. 30, no. 5, pp. 2413–2426, May 2015.

[5] H. Luo, X. Wang, C. Zhu, W. Li, and X. He, "Investigation and emulation of junction temperature for high-power IGBT modules considering grid codes," *IEEE J. Emerg. Sel. Topics Power Electron.*, vol. 6, no. 2, pp. 930–940, Jun. 2018.

[6] H. Luo, W. Li, F. Iannuzzo, X. He, and F. Blaabjerg, "Enabling junction temperature estimation via collector-side thermo-sensitive electrical parameters through emitter stray inductance in high-power IGBT modules," *IEEE Trans. Ind. Electron.*, vol. 65, no. 6, pp. 4724–4738, Jun. 2018.

[7] S. Madhusoodhanan, S. Sandoval, Y. Zhao, M. E. Ware, and Z. Chen, "A highly linear temperature sensor using GaN-on-SiC heterojunction diode for high power applications," *IEEE Trans. Electron Device Lett.*, vol. 38, no. 8, pp. 1105–1108, Aug. 2017.

[8] X. Han and M. Saeedifard, "Junction temperature estimation of SiC MOSFETs based on extended Kalman filtering," in *Proc. IEEE Appl. Power Electron. Conf. Expo.*, San Antonio, TX, USA, Mar. 2018, pp. 1687–1694.

[9] J. Li, A. Castellazzi, M. A. Eleffendi, E. Gurpinar, C. M. Johnson, and L. Mills, "A physical RC network model for electrothermal analysis of a multichip SiC power module," *IEEE Trans. Power Electron.*, vol. 33, no. 3, pp. 2494–2508, Mar. 2018.

[10] H. Luo, W. Li, and X. He, "Online high-power P-i-N diode chip temperature extraction and prediction method with maximum recovery current di/dt," *IEEE Trans. Power Electron.*, vol. 30, no. 5, pp. 2395–2404, May 2015.

[11] A. Griffo, J. Wang, K. Colombage, and T. Kamel, "Real-Time measurement of temperature sensitive electrical parameters in SiC power MOSFETs," *IEEE Trans. Ind. Electron.*, vol. 65, no. 3, pp. 2663–2671, Mar. 2018.

[12] J. O. Gonzalez, O. Alatise, J. Hu, L. Ran, and P. Mawby, "An investigation of temperature sensitive electrical parameters for SiC power MOSFETs," *IEEE Trans. Power Electron.*, vol. 32, no. 10, pp. 7954–7966, Oct. 2017.

[13] F. Stella, G. Pellegrino, E. Armando, and D. Dapra, "On-Line temperature estimation of SiC power MOSFET modules through on-state resistance mapping," in *Proc. IEEE Energy Convers. Congr. Expo.*, Cincinnati, OH, USA, 2017, pp. 5907–5914.

[14] H. Li, X. Liao, Y. Hu, Z. Zeng, E. Song, and H. Xiao, "Analysis of SiC MOSFET dI/dt and its temperature dependence," *IET Power Electron.*, vol. 11, no. 3, pp. 491–500, Mar. 2018.

[15] C. Huifeng, J. Bing, V. Pickert, and C. Wenping, "Real-Time temperature estimation for power MOSFETs considering thermal aging effects," *IEEE Trans. Device Mater. Rel.*, vol. 14, no. 1, pp. 220–228, Mar. 2014.

[16] H. Niu and R. D. Lorenz, "Real-Time junction temperature sensing for silicon carbide MOSFET with different gate drive topologies and different operating conditions," *IEEE Trans. Power Electron.*, vol. 33, no. 4, pp. 3424–3440, Apr. 2018.

[17] E. F. Schubert, *Light-Emitting Diodes*, 2nd ed. Cambridge, U.K.: Cambridge Univ. Press, 2006.

[18] ROHM Semiconductor Application note, SiC Power Devices and Modules Application Note, 2014.

[19] S. Ji, S. Zheng, F. Wang, and L. M. Tolbert, "Temperature-Dependent characterization, modeling, and switching speed-limitation analysis of third-generation 10-kV SiC MOSFET," *IEEE Trans. Power Electron.*, vol. 33, no. 5, pp. 4317–4327, May 2018.

[20] D. Martin, P. Killeen, W. A. Curbow, B. Sparkman, L. E. Kegley, and T. McNutt, "Comparing the switching performance of SiC MOSFET intrinsic body diode to additional SiC schottky diodes in SiC power modules," in *Proc. IEEE Workshop Wide Bandgap Power Devices Appl.*, Fayetteville, AR, 2016, pp. 242–246.

[21] S. Yin, Y. Liu, Y. Liu, K. J. Tseng, J. Pou, and R. Simanjorang, "Comparison of SiC voltage source inverters using synchronous rectification and freewheeling diode," *IEEE Trans. Ind. Electron.*, vol. 65, no. 2, pp. 1051–1061, Feb. 2018.

[22] J. Winkler, J. Homoth, and I. Kallfass, "Utilization of parasitic luminescence from power semiconductor devices for current sensing," in *Proc. PCIM Eur.*, Nuremberg, Germany, May 2018, pp. 1–8.

[23] B. J. Baliga, *Fundamentals of Power Semiconductor Devices*. New York, NY, USA: Springer, 2008.

[24] T. Kimoto, "Material science and device physics in SiC technology for high-voltage power devices," *Jpn. J. Appl. Phys.*, vol. 54, Mar. 2015, Art. no. 040103.

[25] D. A. Neamen, *Semiconductor Physics and Devices: Basic Principles*, 3rd ed. New York, NY, USA: McGraw-Hill, 2003.

[26] L. S. Zhang, J. P. Bergman, N. T. Son, and E. Janzen, "Electrically active defects in n-type 4H–silicon carbide grown in a vertical hotwall reactor," *J. Appl. Phys.*, vol. 93, no. 8, pp. 4708–4714, Apr. 2003.

[27] S. Yin, Y. Liu, Y. Liu, K. J. Tseng, J. Pou, and R. Simanjorang, "Comparison of SiC voltage source inverters using synchronous rectification and freewheeling diode," *IEEE Trans. Ind. Electron.*, vol. 65, no. 2, pp. 1051–1061, Feb. 2018.

[28] P. B. Klein, "Carrier lifetime measurement in n−4H-SiC epilayers," *J. Appl. Phys.*, vol. 103, no. 3, Feb. 2008, Art. no. 033702.

[29] R. N. Hall, "Recombination processes in semiconductors," *Proc. Inst. Elec. Eng.*, vol. 106, no. part B, pp. 923–931, May 1959.

[30] C. J. M. LasanceAndrás Poppe, *Thermal Management for LED Applications*. New York, NY, USA: Springer, 2014.

[31] Y. P. Varshni, "Temperature dependence of the energy gap in semiconductors," *Physica*, vol. 34, no. 1, pp. 149–154, Aug. 1967.

[32] D. Johannesson and M. Nawaz, "Development of a simple analytical PSpice model for SiC-Based BJT power modules," *IEEE Trans. Power Electron.*, vol. 31, no. 6, pp. 4517–4525, Jun. 2016.

[33] Datasheet, SFH250V, Plastic Fiber Optic Photodiode Detector, Infineon, Inc., 2004.[Online]. Available: www.infineon.com

[34] Datasheet, OTG-F, fiber optic temperature sensor, Opsens Solutions, 2015. [Online]. Available: https://opsens-solutions.com/products/fiber-optic-temperature-sensors/otg-f

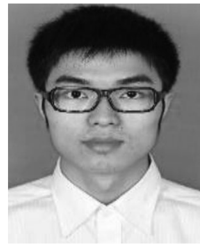

Chengmin Li (S'15) received the B.S. degree in electrical engineering from the School of Electrical and Electronic Engineering, Huazhong University of Science and Technology, Wuhan, China, in 2013. He is currently working toward the Ph.D. degree with the College of Electrical Engineering at Zhejiang University, Hangzhou, China. From March 2016 to March 2017, he was a Research Intern with the GE Global Research Center, Shanghai, China. His research interests include characterization of power devices and applications of SiC power MOSFETs in high power converters.

Haoze Luo (M'15) received the B.S. and M.S. degrees from the Hefei University of Technology, Hefei, China, in 2008 and 2011, respectively. He received the Ph.D. degree from Zhejiang University, Hangzhou, China, in 2015.

From January to April 2015, he was a Visiting Researcher at Newcastle University, Newcastle upon Tyne, U.K. From October 2015 to May 2018, he was a Postdoc at the Department of Energy Technology in Aalborg University, Denmark. His research interests include high-power converters and reliability of high-power modules.

Chushan Li (M'17) received the B.E.E. and Ph.D. degrees in electrical engineering from the Zhejiang University, Hangzhou, China, in 2008 and 2014, respectively.

He is currently an Assistant Professor in Zhejiang University—University of Illinois at Urbana-Champaign Institute, Zhejiang, China. From April to September in 2008, he was an internship student with the Power Application Design Center in National Semiconductor (Hong Kong) Co.Ltd. From December 2010 to October 2011, he was a Visiting Scholar with the FREEDM Center in North Carolina State University. From December 2013 to June 2014, he was a Research Assistant in Hong Kong Polytechnic University. From July 2014 to July 2017, he was a Postdoctoral Fellow in Department of Electrical and Computer Engineering, Ryerson University, Canada. His research interest includes high power density power converter design and ac–dc power conversion.

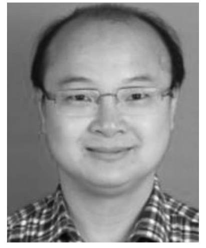

Wuhua Li (M'09) received the B.Sc. and Ph.D. degrees in power electronics and electrical engineering from Zhejiang University, Hangzhou, China, in 2002 and 2008, respectively.

From 2004 to 2005, he was a Research Intern, and from 2007 to 2008, a Research Assistant in GE Global Research Center, Shanghai, China. From 2008 to 2010, he joined the College of Electrical Engineering, Zhejiang University, as a Post Doctor. In 2010, he was promoted as an Associate Professor. Since 2013, he has been a Full Professor at Zhejiang University. From 2010 to 2011, he was a Ryerson University Postdoctoral Fellow with the Department of Electrical and Computer Engineering, Ryerson University, Toronto, ON, Canada. His research interests include power devices, converter topologies, and advanced controls for high power energy conversion systems. He has published more than 200 peer-reviewed technical papers and holds more than 30 issued/pending patents.

Dr. Li, due to his excellent teaching and research contributions, received the 2012 Delta Young Scholar from Delta Environmental and Educational Foundation, the 2012 Outstanding Young Scholar from National Science Foundation of China (NSFC), the 2013 Chief Youth Scientist of National 973 Program, the 2014 Young Top-Notch Scholar of National Ten Thousand Talent Program. He received one National Natural Science Award and four Scientific and Technological Achievement Awards from Zhejiang Provincial Government and the State Educational Ministry of China. He serves as an Associated Editor for *Journal of Emerging and Selected Topics in Power Electronics*, *IET Power Electronics*, *CSEE Journal of Power and Energy Systems*, *Proceedings of the Chinese Society for Electrical Engineering*, a Guest Editor for *IET Renewable Power Generation for Special Issue "DC and HVDC system technologies"*, Member of Editorial Board for Journal of Modern Power System and Clean Energy. He was appointed as the Most Cited Chinese Researchers by Elsevier since 2014.

Huan Yang (M'09) received the B.Sc. and Ph.D. degrees in electrical engineering and its automation and electrical engineering from Zhejiang University, Hangzhou, China, in 2003 and 2008, respectively.

From January 2009 to March 2011, he was a Postdoctoral Fellow at Zhejiang University. In March 2011, he became a faculty member in Zhejiang University as a Research Associate. In December 2012, he became an Associate Professor of electrical engineering at Zhejiang University. From April 2012 to April 2013, he conducted joint research in Fuji Electric Co., Ltd. as the Oversea Researcher of New Energy and Industrial Technology Development Organization (NEDO), Tokyo, Japan. His research interests include distribution generation and microgrids, high performance motor systems, and smart power distribution and consumption equipment. He has published more than 50 papers and holds more than 10 issued/pending patents.

Xiangning He (M'95–SM'96–F'10) received the B.Sc. and M.Sc. degrees from Nanjing University of Aeronautical and Astronautical, Nanjing, China, in 1982 and 1985, respectively, and the Ph.D. degree from Zhejiang University, Hangzhou, China, in 1989.

From 1985 to 1986, he was an Assistant Engineer at the 608 Institute of Aeronautical Industrial General Company, Zhuzhou, China. From 1989 to 1991, he was a Lecturer at Zhejiang University. In 1991, he obtained a Fellowship from the Royal Society of U.K., and conducted research in the Department of Computing and Electrical Engineering, Heriot-Watt University, Edinburgh, U.K., as a Post-Doctoral Research Fellow for two years. In 1994, he joined Zhejiang University as an Associate Professor. Since 1996, he has been a Full Professor in the College of Electrical Engineering, Zhejiang University. He was the Director of the Power Electronics Research Institute, the Head of the Department of Applied Electronics, the Vice Dean of the College of Electrical Engineering, and he is currently the Director of the National Specialty Laboratory for Power Electronics, Zhejiang University. His research interests are power electronics and their industrial applications.

Dr. He was appointed as IEEE Distinguished Lecturer by the IEEE Power Electronics Society in 2011. He is also a Fellow of the Institution of Engineering and Technology (formerly IEE), U.K.